PS Improved Estimation of Water Saturation in a Lower-Paleozoic European Organic-Rich Shale Gas Formation*

Yifu Han[1] and Siddharth Misra[2]

Search and Discovery Article #42154 (2017)**
Posted November 20, 2017

*Adapted from poster presentation given at AAPG 2017 Mid-Continent Section Meeting, Oklahoma City, Oklahoma, September 30 – October 3, 2017

[1]Mewbourne College of Earth and Energy, University of Oklahoma, Norman, OK (misra@ou.edu)
[2]Mewbourne College of Earth and Energy, University of Oklahoma, Norman, OK

Abstract

Unconventional resources or organic-rich shale formation generally exhibits high clay content, significant variations in lithology, rock texture, total organic carbon, accompanied by high connate water salinity, presence of disseminated pyrite grains, and low values of porosity. Subsurface electromagnetic (EM) measurements, namely galvanic resistivity, EM induction, EM propagation, and dielectric dispersion, exhibit frequency dependence due to the interfacial polarization (IP) of clay, grain surfaces, and conductive minerals. These petrophysical attributes adversely affect the log-derived water saturation estimates. The conventional subsurface EM measurement interpretation methods generate inaccurate saturation estimates in clay- and pyrite-bearing shales primarily because multifrequency conductivity and permittivity logs are interpreted separately using empirical models at a single frequency. In this work we propose an inversion-based method to process and interpret broadband EM dispersion logs. In clay and pyrite rich formation, the recently published clay and pyrite dispersion model (PS) is coupled into the inversion scheme to process logs, which takes clay and pyrite IP effects into account.

References Cited

Aster, R.C., B. Borchers, and C.H. Thurber, 2005, Parameter Estimation and Inverse Problems: Elsevier Academic, 320 p.

Han, Y., S. Misra, and G. Simpson, 2017, Dielectric Dispersion Log Interpretation in Bakken Petroleum System: SPWLA 58th Annual Logging Symposium, Oklahoma City, Oklahoma, June 17-21.

Hizem, M., H. Budan, B. Deville, O. Faivre, L. Mosse, and M. Simon, 2008, Dielectric Dispersion – A New Wireline Petrophysical Measurement: SPE Annual Technical Conference and Exhibition, Denver, Colorado, September 21-24, SPE 116130, 21 p.

Misra, S., C. Torres-Verdín, A. Revil, J. Rasmus, and D. Homan, 2016a, Interfacial Polarization of Disseminated Conductive Minerals in Absence of Redox-Active Species - Part 1: Mechanistic Model and Validation: Geophysics, v. 81/2, p. E139-E157.

Misra, S., C. Torres-Verdín, A. Revil, J. Rasmus, and D. Homan, 2016b, Interfacial Polarization of Disseminated Conductive Minerals in Absence of Redox-Active Species - Part 2: Effective Electrical Conductivity and Dielectric Permittivity: Geophysics, v. 81/2, p. E159-E176.

Wang, H., and A. Poppitt, 2013, The Broadband Electromagnetic Dispersion Formation Logging Data in a Gas Shale Formation - A Case Study: SPWLA 54th Annual Logging Symposium, New Orleans, Louisiana, June 22-26.

Improved Estimation of Water Saturation in a Lower-Paleozoic European Organic-Rich Shale Gas Formation

Yifu Han and Siddharth Misra

Mewbourne College of Earth and Energy, The University of Oklahoma

Summary

Unconventional resources or organic-rich shale formation generally exhibits high clay content, significant variations in lithology, rock texture, total organic carbon, accompanied by high connate water salinity, presence of disseminated pyrite grains, and low values of porosity. Subsurface electromagnetic (EM) measurements, namely galvanic resistivity, EM induction, EM propagation, and dielectric dispersion, exhibit frequency dependence due to the interfacial polarization (IP) of clay, grain surfaces, and conductive minerals. These petrophysical attributes adversely affect the log-derived water saturation estimates. The conventional subsurface EM measurement interpretation methods generate inaccurate saturation estimates in clay- and pyrite-bearing shales primarily because multifrequency conductivity and permittivity logs are interpreted separately using empirical models at a single frequency. In this work we propose an inversion-based method to process and interpret broadband EM dispersion logs. In clay and pyrite rich formation, the recently published clay and pyrite dispersion model (PS) is coupled into the inversion scheme to process logs, which takes clay and pyrite IP effects into account.

Introduction

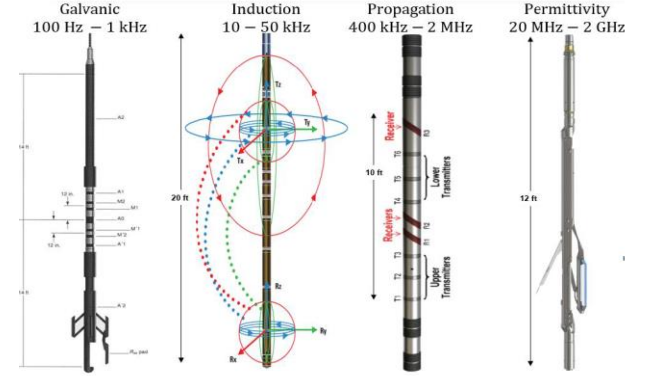

Figure 1. Downhole EM tools (Hizem et al., 2008).

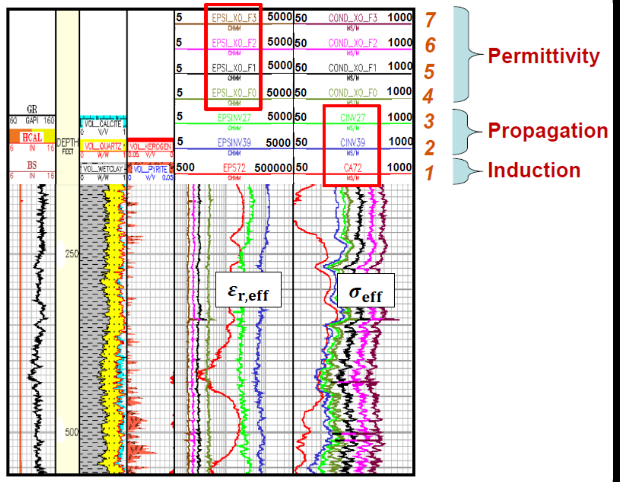

Figure 2. Frequency dispersion conductivity and permittivity logs (Wang and Poppitt, 2013).

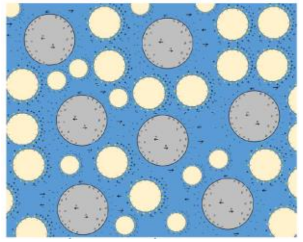

Figure 3. The alteration in electromigration (Misra et al., 2016).

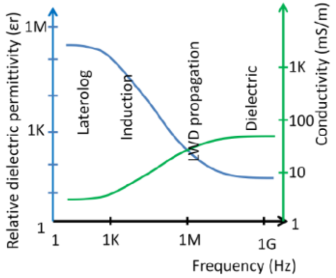

Figure 4. The characteristics of EM dispersion of sedimentary rock as a function of frequency (Wang and Poppitt, 2013).

Inversion

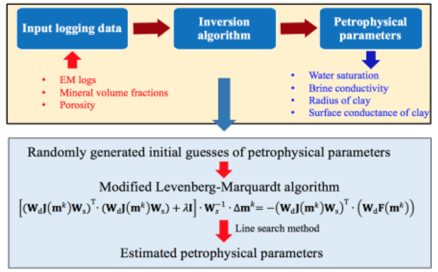

Figure 5. Modified inversion of broadband EM dispersion logs.

Table 1. Assumed petrophysical properties of the synthetic layer used for this study.

Parameters	Unit	Layer
Volume fraction of pyrite grains, V_i	%	5
Bulk conductivity of pyrite, S_i	S/m	1000
Relative permittivity of pyrite, ε_{ri}		30
Diffusion coefficient of pyrite, D_i	m^2/s	10^{-6}
Radius of pyrite grains, r_i	μm	30
Volume fraction of clay, V_c	%	30
Relative permittivity of clay, ε_{rc}		5
Surface conductance of clay, λ_c	S	5×10^{-6}
Radius of spherical clay grains, r_c	μm	0.3
Volume fraction of sand, V_s	%	45
Surface conductance of sand, λ_s	S	10^{-9}
Radius of sand grains, r_s	μm	500
Porosity of rock, φ	%	20
Bulk conductivity of brine, C_w	S/m	3
Relative permittivity of brine, ε_{rb}		80
Diffusion coefficient of brine, D_b	m^2/s	10^{-9}
Relative permittivity of hydrocarbon, ε_{rhy}		3
Water saturation, s_w	%	20

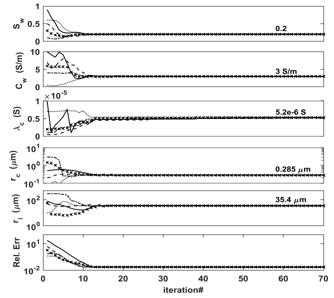

Figure 6. Convergence of modified LMA estimates of PS-model parameters.

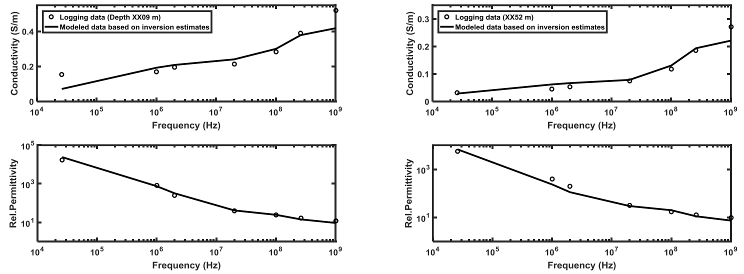

Figure 7. Comparison of measured and modeled broadband dispersion data.

Table 2. Assumed and inversion-derived petrophysical properties for two depths in the organic-rich formation.

Parameters	Unit	Depth XX52	Depth XX09
Volume fraction of pyrite grains, V_i	%	0	2.3
Bulk conductivity of pyrite, S_i	S/m		1000
Relative permittivity of pyrite, ε_{ri}			30
Diffusion coefficient of pyrite, D_i	m^2/s		1×10^{-5}
Radius of pyrite grains, r_i	μm		172
Volume fraction of clay, V_c	%	60	47
Relative permittivity of clay, ε_{rc}		6	6
Surface conductance of clay, λ_c	S	6.6×10^{-8}	2.5×10^{-8}
Radius of spherical clay grains, r_c	μm	0.13	0.1
Volume fraction of sand, V_s	%	31	43
Surface conductance of sand, λ_s	S	10^{-9}	10^{-9}
Radius of sand grains, r_s	μm	500	500
Porosity of rock, φ	%	9	7.7
Bulk conductivity of brine, C_w	S/m	0.48	0.38
Relative permittivity of brine, ε_{rb}		80	80
Diffusion coefficient of brine, D_b	m^2/s	1.5×10^{-9}	1.5×10^{-9}
Relative permittivity of hydrocarbon, ε_{rhy}		3	3
Water saturation, s_w	%	100	46

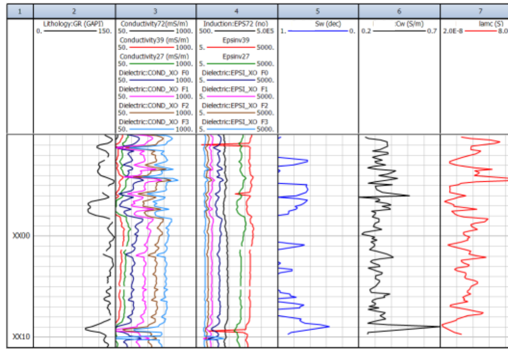

Figure 8. Inversion-derived estimates of water saturation, brine conductivity, surface conductance of clay, and radius of clay presented in Track 5, Track 6, Track 7 and Track 8, respectively.

Conclusions

Improved water saturation estimates were obtained in one shale gas well in an European Lower Paleozoic formation. This mandates application of the newly proposed inversion scheme on multifrequency permittivity and conductivity logs, generally obtained by running EM induction, propagation, and dielectric dispersion tools in a single well. The proposed method ensures consistent estimation of water saturation and certain petrophysical parameters irrespective of the EM log-acquisition frequency which is extremely beneficial for shales rich in clay and pyrite.

Contact

Yifu Han

Mewbourne College of Earth and Energy, The University of Oklahoma

Email: yifu@ou.edu

References

Aster, R., B. Borchers, and C. Thurber, 2005, Parameter estimation and inverse problems: Elsevier Academic.

Han, Y., S. Misra, and G. Simpson, 2017, Dielectric dispersion log interpretation in Bakken Petroleum System: Presented at the 58th Annual Logging Symposium, SPWLA.

Hizem, M., H. Budan, B. Deville, O. Faivre, L. Mosse, and M. Simon, 2008, Dielectric Dispersion – A new wireline petrophysical measurement: Presented at the Annual Technical Conference and Exhibition, SPE.

Misra, S., C. Torres-Verdín, A. Revil, J. Rasmus, and D. Homan, 2016a, Interfacial polarization of disseminated conductive minerals in absence of redox-active species—Part 1: Mechanistic model and validation: Geophysics, **81**(2), E139-E157.

Misra, S., C. Torres-Verdín, A. Revil, J. Rasmus, and D. Homan, 2016b, Interfacial polarization of disseminated conductive minerals in absence of redox-active species—Part 2: Effective electrical conductivity and dielectric permittivity: Geophysics, **81**(2), E159-E176.

Wang, H., and A. Poppitt, 2013, The broadband electromagnetic dispersion logging data in a gas shale formation: a case study: Presented at the 54th Annual Logging Symposium, SPWLA